

East African Journal of Environment and Natural Resources

eajenr.eanso.org

Volume 6, Issue 1, 2023

Print ISSN: 2707-4234 | Online ISSN: 2707-4242

Title DOI: <https://doi.org/10.37284/2707-4242>

EANSO

EAST AFRICAN
NATURE &
SCIENCE
ORGANIZATION

Original Article

Estimating Seasonal and Interannual Variations in Precipitation in Rural Eastern Africa: A Case Study in Longido, Tanzania

Anoopa Susan Kuriakose¹, Thomas William Walker^{1*} & Onita Basu¹

¹ Carleton University, Ottawa, ON, K1S 5B6, Canada.

* Correspondence ORCID ID: <https://orcid.org/0000-0001-9065-7361>; email: thomas.walker@carleton.ca

Article DOI: <https://doi.org/10.37284/eajenr.6.1.1242>

Date Published: ABSTRACT

07 June 2023

Keywords:

*Precipitation,
Water Resources,
Remote Sensing,
Climate Change,
Time Series Analysis*

Access to water is a limiting factor for development in many semi-arid regions, contributing to food insecurity and environmental stresses on the local population. Additionally, some rural areas still have limited quantitative data on weather and associated rainfall patterns. This study analyzes ground meteorological data from a station installed at Longido, Tanzania and performs time series decomposition modelling of complementary Integrated Multi-satellite Retrievals (IMERG) data to quantify the amount, distribution, and variability of this essential resource. The seasonal rainfall pattern at Longido is bimodal with a large peak between March and May and a smaller peak between October and November. Interannual variability in rainfall is only weakly correlated with El Niño and the Indian Ocean Dipole indices; however, the highest observed rainfall does occur in a year with numerous simultaneous storms in the southern Indian Ocean. This analysis will help improve water management planning in the locality and points to a need to promote and support water storage as a method to meet the needs of the local population.

APA CITATION

Kuriakose, A. S., Walker, T. W. & Basu, O. (2023). Estimating Seasonal and Interannual Variations in Precipitation in Rural Eastern Africa: A Case Study in Longido, Tanzania. *East African Journal of Environment and Natural Resources*, 6(1), 151-165. <https://doi.org/10.37284/eajenr.6.1.1242>.

CHICAGO CITATION

Kuriakose, Anoopa Susan, Thomas William Walker and Onita Basu. 2023. "Estimating Seasonal and Interannual Variations in Precipitation in Rural Eastern Africa: A Case Study in Longido, Tanzania". *East African Journal of Environment and Natural Resources* 6 (1), 151-165. <https://doi.org/10.37284/eajenr.6.1.1242>.

HARVARD CITATION

Kuriakose, A. S., Walker, T. W. & Basu, O. (2023) "Estimating Seasonal and Interannual Variations in Precipitation in Rural Eastern Africa: A Case Study in Longido, Tanzania", *East African Journal of Environment and Natural Resources*, 6 (1), pp. 151-165. doi: 10.37284/eajenr.6.1.1242.

IEEE CITATION

A. S., Kuriakose, T. W., Walker & O., Basu. "Estimating Seasonal and Interannual Variations in Precipitation in Rural Eastern Africa: A Case Study in Longido, Tanzania", *EAJENR*, vol. 6, no. 1, pp. 151-165, Jun. 2023.

MLA CITATION

Kuriakose, Anoop Susan, Thomas William Walker & Onita Basu. "Estimating Seasonal and Interannual Variations in Precipitation in Rural Eastern Africa: A Case Study in Longido, Tanzania". *East African Journal of Environment and Natural Resources*, Vol. 6, no. 1, Jun 2023, pp. 151-165, doi:10.37284/eajenr.6.1.1242.

INTRODUCTION

Water availability across Africa is a pressing issue (Mkonda and He, 2018) as the frequency of both drought events and bouts of intense precipitation on the continent will likely increase under climate change (Bates et al., 2008; Lyon, 2014; Ogwang et al., 2019). Rural sub-Saharan Eastern Africa presents particular challenges for estimating water availability due to (i) the interactions between the complex topography, the tropical jet circulations, and the distribution of rainfall (Matayo et al., 2000; Chakraborty et al., 2009), (ii) the dependence of pastoral and agrarian communities on rainfall collection (Mkonda and He, 2018), and (iii) the limited number of high-quality meteorological measurements in these rural communities. Knowledge of the interannual and seasonal variability in precipitation amount and intensity in rural sub-Saharan Eastern Africa is a crucial element for resource management, for example, in planning water collection and storage requirements.

The annual progression of rainfall in sub-Saharan Eastern Africa exhibits two peaks. The first has a greater magnitude and occurs between March and May and is known as the "long rain" season. This is followed by a long dry period in the boreal summer months, which is followed by the "short rain" season that occurs between October and December. This progression is in phase with sea-surface temperatures (SSTs) in the Western Equatorial Indian Ocean (Yang et al., 2015). The circulations underlying the rainy seasons in sub-Saharan Eastern Africa are created by a combination of the north-south movement of the Intertropical Convergence Zone (ITCZ) throughout the year (Slingo et al., 2005) and the regional topography channelling a series of low-level jets (Chakraborty et al., 2009; Nicholson, 2016). The origin of these jet circulations is connected to the Asian monsoon and

its effects on the Tropical Easterly Jet (Slingo et al., 2005; Nicholson and Klotter, 2020).

Several climate studies in sub-Saharan Eastern Africa have attempted to relate precipitation patterns to large-scale flow features in attempts to better understand or even predict annual precipitation. Mechanistic links between the SSTs in the Indian Ocean, the Asian monsoonal circulation, the Tropical Easterly Jet, and precipitation in the Sahel region have been studied (Dyer et al., 2017; Nicholson and Klotter, 2020). Analysis of the CMIP5 climate model ensemble has identified feedback between the long rain season in sub-Saharan Eastern Africa and SSTs in the southern Indian Ocean (Rowell, 2019). Exploiting these teleconnections by understanding the climate processes involved can lead to improvements in prediction capacity, as has been shown for the Asian summer monsoon (Takaya et al., 2021).

Weather station data in remote areas can be challenging to maintain over a long time period (3-5 years or longer). Thus, this research attempts to supplement weather station data with remote sensing observations, first to establish the reliability of satellite data to estimate local precipitation and then to describe the regionalized context of weather and rainfall data. This highlights the strength of combining ground-based and satellite data in areas where access to ground-based data is limited. Ultimately, this can assist with water management and planning to help adapt to climate change.

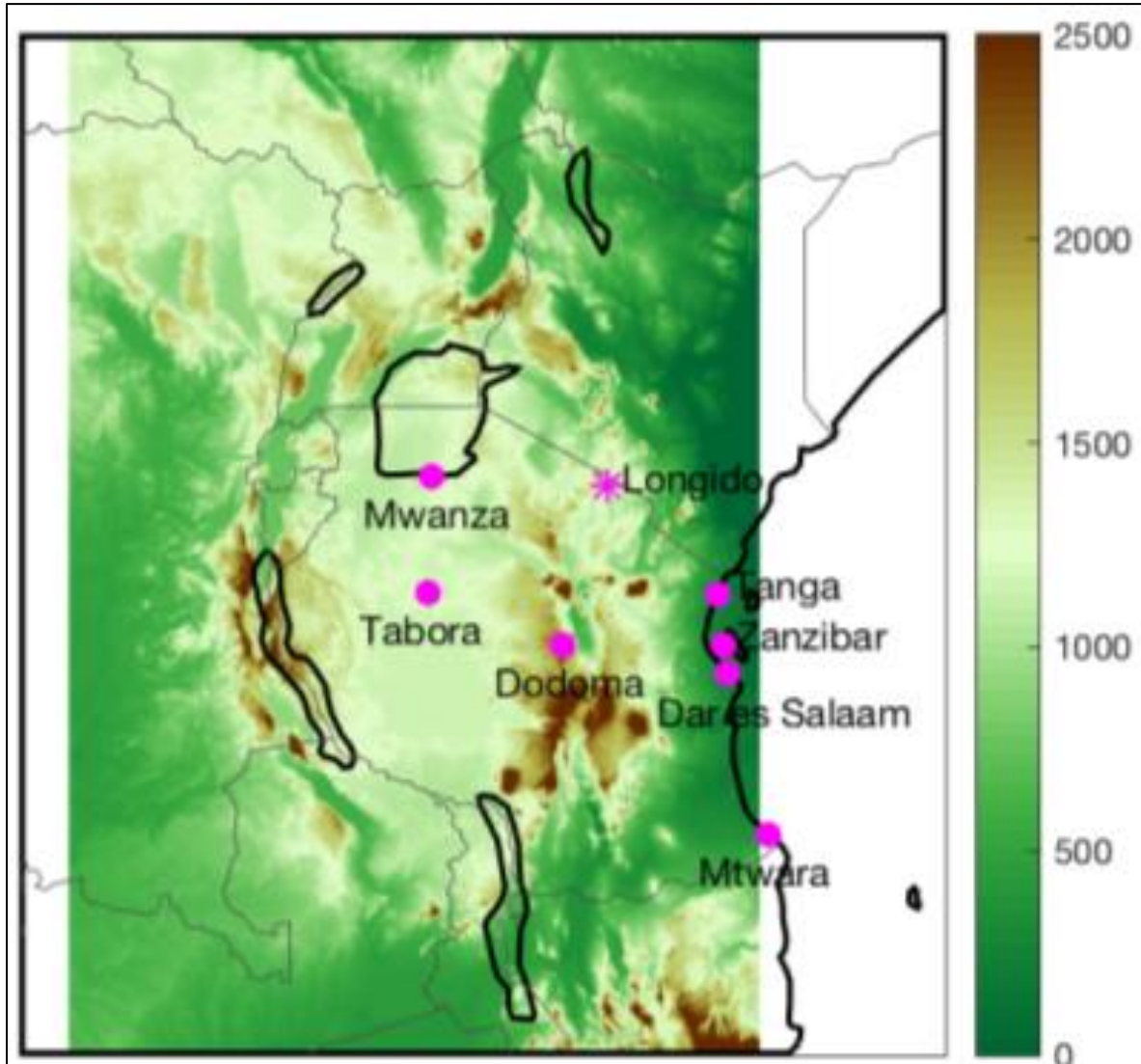
METHODS AND MATERIALS**Meteorological Measurements in Longido, Tanzania**

A weather station (David Instruments) installed by researchers from Carleton University in 2015 at Longido in the Arusha region of Tanzania (2.75° S,

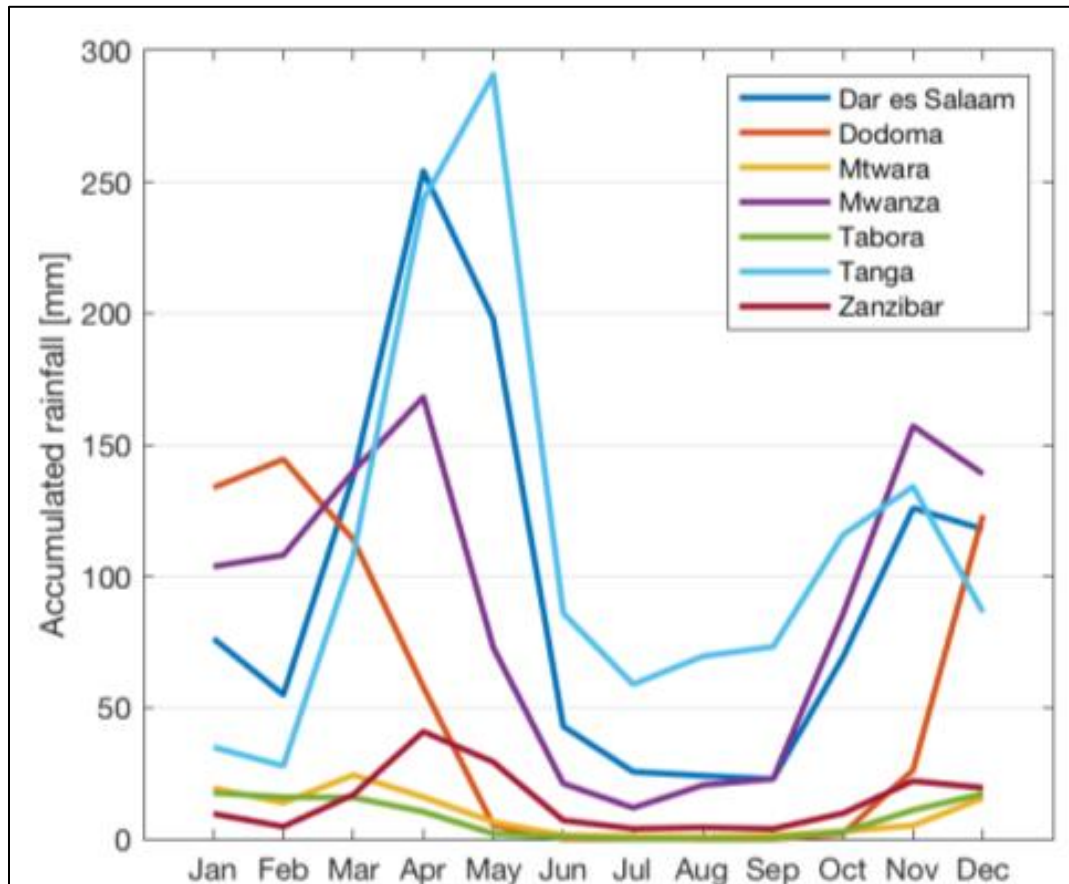
36.65° E) will serve as a source of ground measurements for intercomparison with other meteorological data and trends when possible and as a means of helping the local community plan rainwater collection efforts. Longido is a small community near the Tanzania-Kenya border in the highlands to the northwest of Mount Kilimanjaro

(see *Figure 1*). The weather station includes instruments measuring temperature, humidity, wind speed and direction, pressure, and precipitation; we primarily use hourly precipitation data. This data is sparse due to hardware issues, and the data is only available from 2016 to 2019.

Figure 1: Map of locations of WMO ground stations in Tanzania



Coloured shading represents elevation (in m). The location of Longido is marked with a star

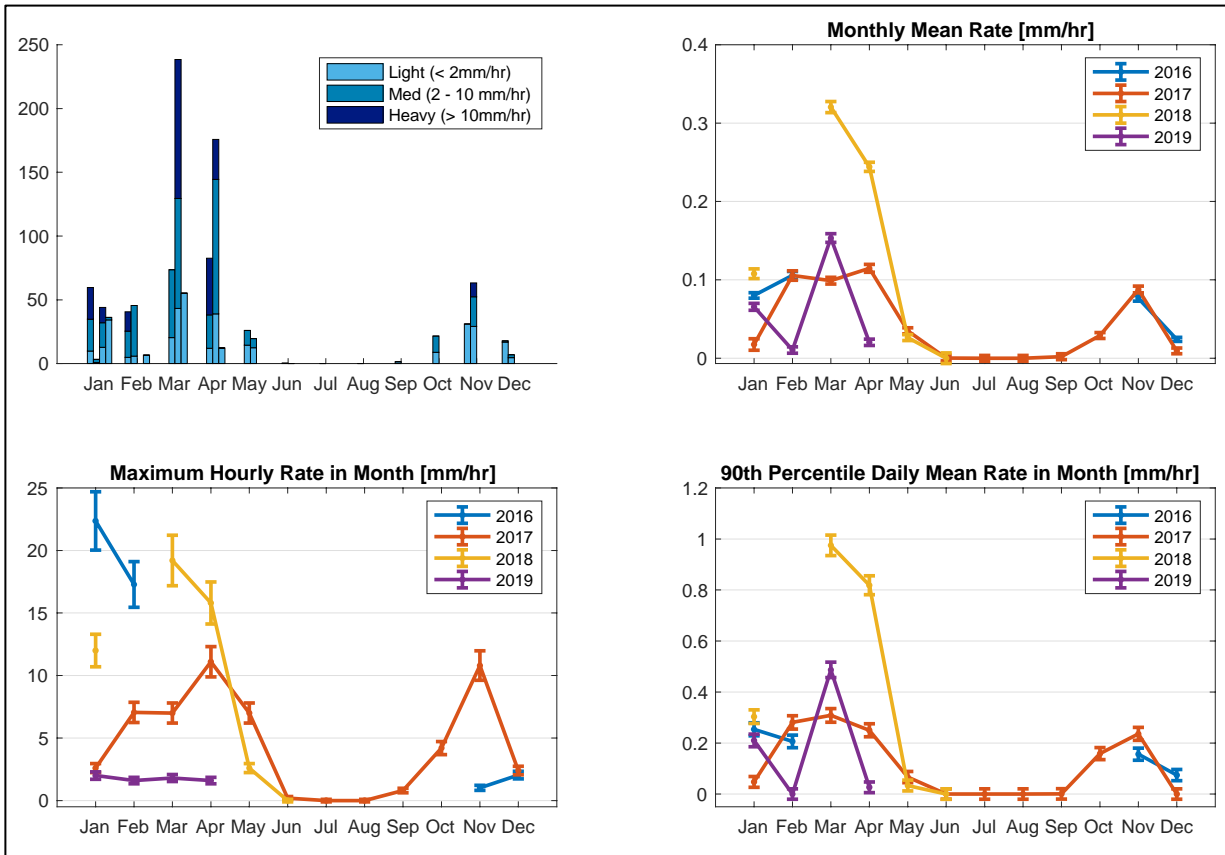
Figure 2: The climatological monthly rainfall accumulation from 1981-2010 at each station (in mm)

Visual inspection of hourly data does not show evidence of truncation at heavy precipitation values, a common data quality problem with precipitation measurements (Hunziker et al., 2017). However, there is likely the presence of sampling error in the measurements, which will be large in a region like Arusha, which is a warm region subject to short, high-intensity storms (Walker et al., 2016). The low gauge density in the region also precludes spatial consistency checks. Investing in local personnel in the region for training and the implementation of routine quality control measures can help alleviate some of these data quality issues.

Monthly rainfall statistics were calculated from the precipitation data. Days having > 80% valid hourly

measurements were kept in the analysis, and monthly statistics were only calculated for months with > 25% valid days. Each hourly rainfall measurement was presumed to have an uncertainty of 10% plus 0.1 mm to attempt to capture instrument uncertainty and spatial and temporal sampling errors. The monthly accumulation, monthly mean rainfall rate, monthly maximum hourly rate, and 90th percentile of the daily mean rainfall rate in each month were computed and are displayed in *Figure 3*. The numeric values and their accumulated uncertainties are also summarized in *Tables 1* and *2*. Further discussion on this data is found in the Results and Discussion section.

Figure 3: Monthly rainfall accumulation (in mm, top left) and rainfall rate statistics at the ground station in Longido, Tanzania



Key: Monthly values for the mean monthly rate (in mm/hr, top right), maximum hourly rate within the month (in mm/hr, bottom left), and the 90th percentile of the daily mean rates in the month (in mm/hr, bottom right) are displayed for the four years of data collection. Data points are plotted only for months where >25% of the days in the month have >80% of the hourly measurements in the day. Error bars represent accumulated measurement uncertainty.

Table 1: Monthly precipitation statistics measured at a weather station in Longido, Tanzania from January to June. A dash indicates insufficient data for the month (see text for details).

Year	Variable	Jan	Feb	Mar	Apr	May	Jun
2016	Monthly Accum. [mm]	60 ± 1	41 ± 1	-	-	-	-
	Valid Days	31	16	0	0	0	0
	Monthly Mean Rate [μm /hr]	80 ± 3	106 ± 5	-	-	-	-
	Max. Hourly rate [mm/hr]	22 ± 2	17 ± 2	-	-	-	-
	90th Perc. Daily rate [μm /hr]	250 ± 30	210 ± 30	-	-	-	-
2017	Monthly Accum. [mm]	3.6 ± 0.2	46 ± 1	74 ± 1	83 ± 2	26.0 ± 0.5	0.20 ± 0.02
	Valid Days	8	18	31	30	31	30
	Monthly Mean Rate [μm /hr]	18 ± 7	106 ± 16	99 ± 4	115 ± 5	35 ± 4	0 ± 4
	Max. Hourly rate [mm/hr]	2.6 ± 0.4	7.1 ± 0.8	7.0 ± 0.8	11 ± 1	7.0 ± 0.8	0.2 ± 0.1
	90th Perc. Daily rate [μm /hr]	50 ± 20	280 ± 30	310 ± 30	250 ± 30	70 ± 20	0 ± 20
2018	Monthly Accum. [mm]	44 ± 1	-	238 ± 4	176 ± 3	19.6 ± 0.4	0.00 ± 0.03
	Valid Days	17	5	31	30	31	9
	Monthly Mean Rate [μm /hr]	108 ± 6	-	320 ± 7	244 ± 6	26 ± 4	0 ± 7
	Max. Hourly rate [mm/hr]	12 ± 1	-	19 ± 2	16 ± 2	2.6 ± 0.4	0.0 ± 0.1
	90th Perc. Daily rate [μm /hr]	300 ± 30	-	980 ± 40	820 ± 40	0 ± 20	0 ± 20
2019	Monthly Accum. [mm]	36.2 ± 0.8	6.6 ± 0.1	55 ± 2	12.2 ± 0.3	-	-
	Valid Days	23	26	15	25	0	0
	Monthly Mean Rate [μm /hr]	66 ± 4	11 ± 4	153 ± 6	20 ± 4	-	-
	Max. Hourly rate [mm/hr]	2.0 ± 0.3	1.6 ± 0.3	1.8 ± 0.3	1.6 ± 0.3	-	-
	90th Perc. Daily rate [μm /hr]	210 ± 30	0 ± 20	490 ± 30	30 ± 20	-	-

Table 2: Monthly precipitation statistics measured at a weather station in Longido, Tanzania from July to December. A dash indicates insufficient data for the month (see text for details).

Year	Variable	Jul	Aug	Sep	Oct	Nov	Dec
2016	Monthly Accum. [mm]	-	-	-	-	31.1 ± 0.8	17.9 ± 0.3
	Valid Days	0	0	0	0	17	31
	Monthly Mean Rate [$\mu\text{m/hr}$]	-	-	-	-	76 ± 4	24 ± 3
	Max. Hourly rate [mm/hr]	-	-	-	-	1.0 ± 0.2	2.0 ± 0.3
	90th Perc. Daily rate [$\mu\text{m/hr}$]	-	-	-	-	160 ± 20	70 ± 20
2017	Monthly Accum. [mm]	0.00 ± 0.02	0.00 ± 0.02	1.40 ± 0.04	21.6 ± 0.4	63 ± 1	7.0 ± 0.1
	Valid Days	31	31	30	31	30	31
	Monthly Mean Rate [$\mu\text{m/hr}$]	0 ± 4	0 ± 4	2 ± 4	29 ± 4	88 ± 4	9 ± 4
	Max. Hourly rate [mm/hr]	0.0 ± 0.1	0.0 ± 0.1	0.8 ± 0.2	4.2 ± 0.5	11 ± 1	2.4 ± 0.3
	90th Perc. Daily rate [$\mu\text{m/hr}$]	0 ± 20	0 ± 20	0 ± 20	160 ± 20	240 ± 30	0 ± 20
2018	Monthly Accum. [mm]	-	-	-	-	-	-
	Valid Days	0	1	1	0	1	0
	Monthly Mean Rate [$\mu\text{m/hr}$]	-	-	-	-	-	-
	Max. Hourly rate [mm/hr]	-	-	-	-	-	-
	90th Perc. Daily rate [$\mu\text{m/hr}$]	-	-	-	-	-	-
2019	Monthly Accum. [mm]	-	-	-	-	-	-
	Valid Days	0	0	0	0	0	0
	Monthly Mean Rate [$\mu\text{m/hr}$]	-	-	-	-	-	-
	Max. Hourly rate [mm/hr]	-	-	-	-	-	-
	90th Perc. Daily rate [$\mu\text{m/hr}$]	-	-	-	-	-	-

Satellite Precipitation Measurements

Precipitation retrievals from NASA's Global Precipitation Measurement (GPM) mission were analyzed, specifically the Integrated Multi-satellite Retrievals (IMERG) product, v6 (Huffman et al., 2019b). GPM is an international collaborative mission between NASA and the Japan Aerospace Exploration Agency (JAXA) that combines information from multiple satellite instruments orbiting Earth to collect rain, snow, and other precipitation data with broad spatial coverage every thirty minutes. The GPM Core Observatory was launched in Japan in 2014 (Hou et al., 2014). It carries the first space-borne Dual-Frequency Precipitation Radar (DPR) with channels in the Ku-band (35.5 GHz) and Ka-band (13.6 GHz) and a conical scanning multichannel microwave imager, the GPM Microwave Imager (GMI). Together, these instruments provide a powerful synergistic tool to assess the small and large-scale structures of precipitation, including its intensity and phase globally at relatively high spatial resolution (Skofronick-Jackson et al., 2018). The DPR provides information on 3D precipitation (rain and snow) particle structure with a vertical resolution of 250 m and a horizontal resolution of about 5 km, while GMI provides data to estimate surface precipitation at resolutions ranging from 5 to 25 km depending on frequency (Hou et al., 2014).

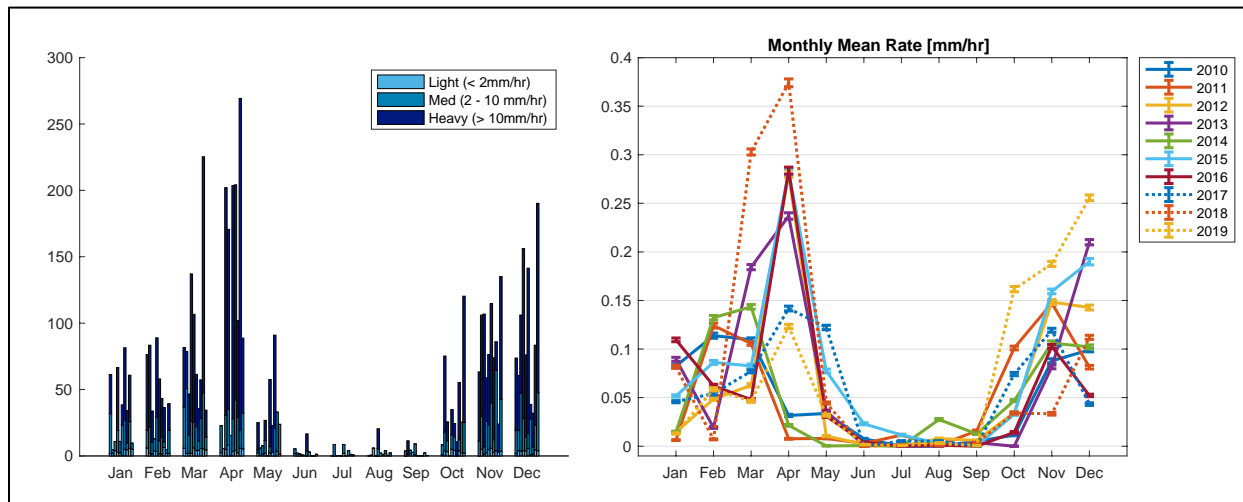
The IMERG product supplements the GPM Core Observatory with observations from other low Earth orbit (LEO) satellites of opportunity that carry passive microwave (PMW) instruments for estimating precipitation and with geostationary Earth orbit (GEO) satellites of opportunity that carry infrared (IR) instruments for the same (Huffman et al., 2019a). PMW instrument estimates of precipitation are interpolated and augmented using IR estimates where data coverage is sparse due to the limitations of the LEO geometry. PMW instruments are further used to calibrate the precipitation estimates from IR instruments. This

permits the IMERG record to calculate a single calibrated, continuous, long-term dataset of precipitation.

IMERG precipitation estimates have previously been evaluated against dense precipitation gauge networks, exhibiting a normalized RMS error of less than 1.79 mm against WegenerNet data in Austria (O et al., 2017). Interestingly, the same study observed IMERG assigning larger values of precipitation to less intense events, biasing the cumulative distribution at low rainfall intensities. Collocated comparisons between gauge networks, ground-based radar, and IMERG in the southern US show good spatial consistency and reasonable temporal consistency among the three methods (Li et al., 2020). However, the latter study focused on hurricanes and other high-intensity rainfall events, so biases at low rainfall rates were not noted. IMERG did outperform the gauge networks in this case, but mainly due to the saturation of the gauges during high-intensity events.

Figure 4 displays ten years of IMERG v6 data at Longido (2.75° S, 36.65° E), which was obtained at a spatial resolution of 0.1° × 0.1° (Huffman et al., 2019b). Daily IMERG data were aggregated into monthly accumulation and mean monthly rate statistics for comparison with the rain gauge data. Similar to previous studies that compare IMERG estimates to rain gauges (e.g., O et al. (2017); Gilewski and Nawalany (2018)), we find that IMERG data is capable of reproducing the relative shape and timing of the rainfall seasonality captured by the ground station data, although discrepancies appear in the precise magnitude of the peak values. For example, the year 2018 in both datasets contains the highest monthly mean rates on record, higher than 0.3 mm/hr, but the satellite estimates show a higher value in April compared to March, while the ground data shows the inverse. The April 2018 satellite estimate of the mean monthly rate is 53% higher than that recorded from the ground.

Figure 4: IMERG estimates of monthly precipitation accumulation (in mm, left) and mean rainfall rate (in mm/hr, right) at Longido, Tanzania from 2010 to 2019.



Over a ten-year record from 2010 to 2019, annual accumulation estimated by IMERG ranged from 420 mm (in 2010) to 730 mm (in both 2015 and 2018) with a mean of 560 mm. The two heavy rainfall years differ in the timing of the rainfall in that the long rain season in 2015 was shorter than in 2018, and the 2015 short rain season was more intense. This is consistent with the high degree of variability in the timing and intensity of rainfall observed at the ground station.

RESULTS AND DISCUSSION

Comparison of Ground and Satellite Precipitation Measurements

Due to the short duration and data gaps present in the ground station record, we attempt to situate it within a regional context of contemporary measurements, including the long-term weather World Meteorological Organization (WMO) stations located generally in nearby urban centres. The ground data from Longido is then compared against estimates from the IMERG retrieval to link the long-term, consistent satellite record to the shorter-duration ground station data.

Figure 1 and *2* demonstrates the regional variability of rainfall within Tanzania, using data from the 1981 to 2010 WMO climatological normals at

stations within the country. Most of the country experiences the “long rain” season from about March to May, followed by a number of extremely dry months, and then a “short rain” season from about October to December. However, the amount of rainfall in these wet seasons varies markedly from location to location, with coastal regions receiving a significantly greater amount than those farther inland. The exception to this is the Mwanza station located on the coast of Lake Victoria, which has been shown to have a significant impact on the local climate (Thiery et al., 2015).

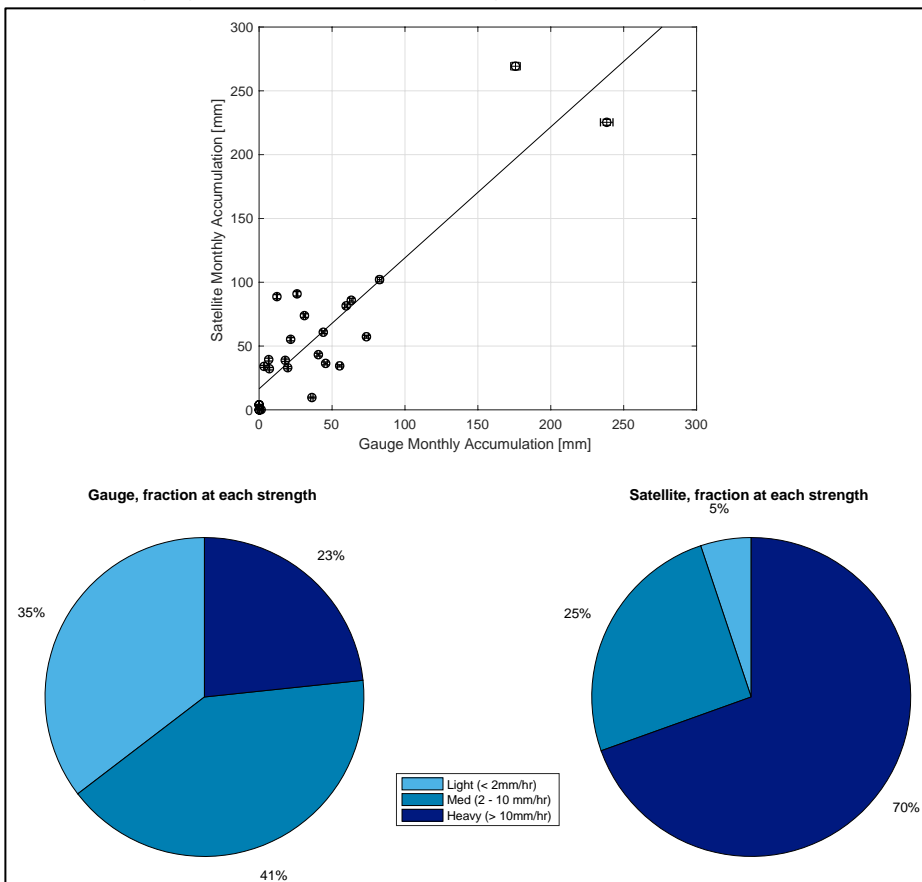
The Longido ground data displays an evident seasonality, with the largest rainfall accumulations occurring within the “long rain” season in March and April. This is followed by a dry period from roughly June through September and then smaller rainfall accumulations during the “short rain” season from October to December. *Figure 3* shows high variability from year to year in the long rain season in the mean, maximum hourly rate, and 90th percentile daily mean rate. The total accumulation during the long rain season (from March to May) in 2017 was 183 ± 2 mm, while the following year, it had more than doubled to 434 ± 5 mm. The total amount of rain falling in a season is significantly variable even across this short measurement period, as are the timing and intensity of the individual

rainfall events themselves – the highest maximum hourly rainfall rate recorded occurred in January 2016 at 22 ± 2 mm/hr, which exceeds any hourly rate recorded in the first four months of 2019 by more than a factor of ten. The capricious timing and intensity of rainfall at Longido encourage examination over a longer timescale.

The IMERG product provides a consistent long-term record for comparison; however, it is worthwhile examining the satellite-derived product for bias relative to the ground data. *Figure 5* shows a least squares linear fit through the scatter of available gauge- and satellite-based monthly accumulation estimates that produce a slope of 1.03 (95% confidence interval 0.80 to 1.25) and intercept of 16.45 (0.78 to 32.12). This suggests the satellite

estimates have a high bias relative to the ground data, consistent with previous intercomparison studies where IMERG tended to overestimate low rainfall rates (O et al., 2017; Gilewski and Nawalany, 2018). The breakdown into light (0 to 2 mm/hr), medium (2 to 10 mm/hr), and heavy (> 10 mm/hr) rainfall rates suggest that IMERG attributes a much greater fraction of the total rain falling in this location to heavy rainfall events, while the rain gauge captures more light and medium rainfall events. More specifically, the monthly rainfall accumulation produced by IMERG is reasonably matched to the rain gauge; however, within the month, the satellite product captures fewer rainfall events but with higher rainfall rates than are observed at the ground site.

Figure 5: Comparison of monthly rainfall accumulation estimated by daily IMERG estimates of hourly rain gauge measurements at Longido, Tanzania from 2016 to 2019



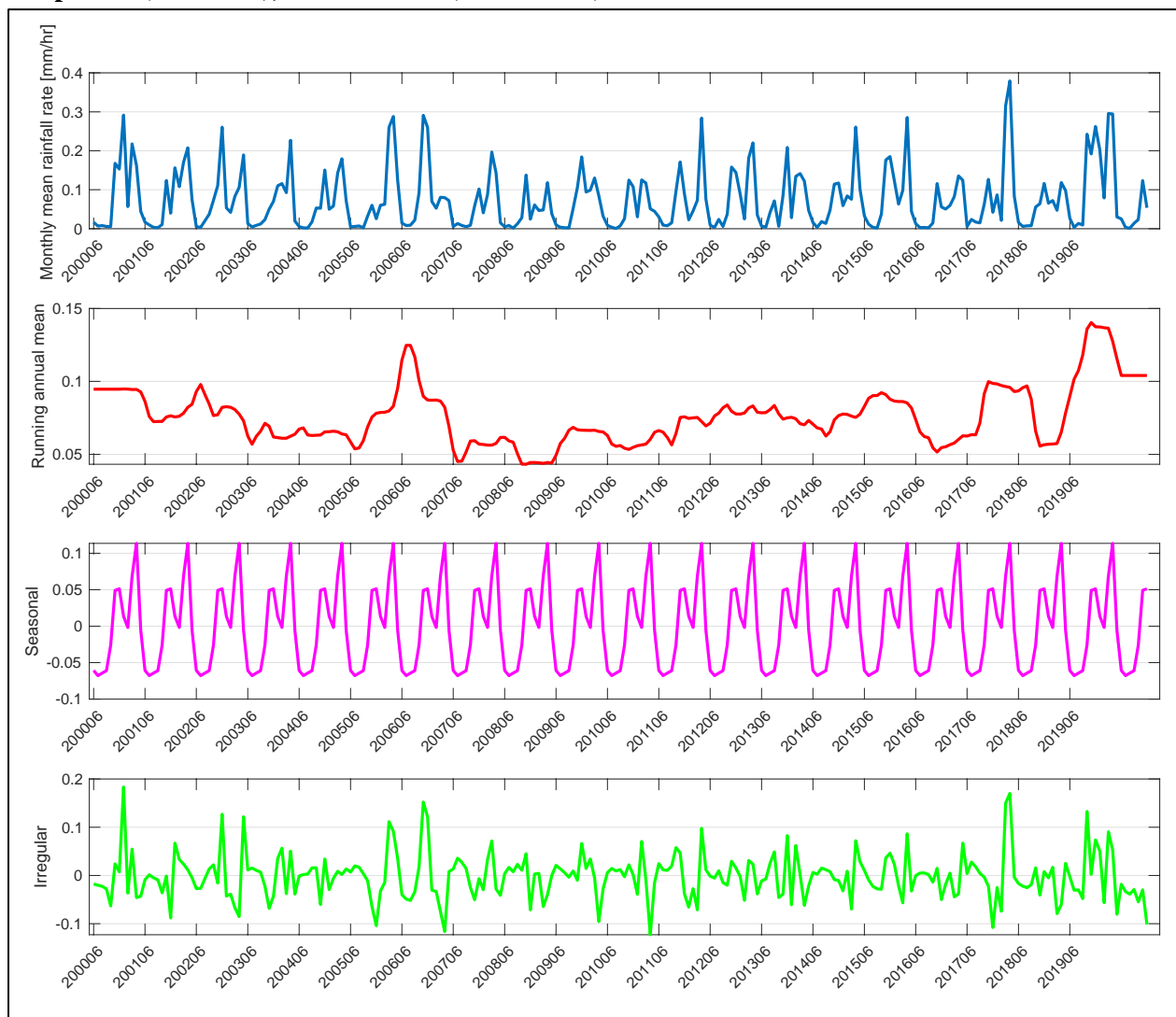
Key: The line of best fit is shown where $r_{IMERG} = 1.03r_{gauge} + 16.5$. The partitioning of rainfall into light, medium, and heavy modes as captured by each instrument, is shown in the pie charts.

Time Series Decomposition of Precipitation at Longido

The IMERG data at monthly resolution shows a small positive bias and a tendency to overestimate the fraction of precipitation from heavy rainfall events. Nevertheless, we decompose the long record of observations in Eastern Africa to fully examine rainfall trends in the region. A time series model was constructed from the monthly precipitation accumulation from IMERG at Longido, Tanzania from 2000 to 2020, which is shown in *Figure 6*. The

time series is decomposed into a 12-month running mean, a seasonally repeating component, and the residuals of the observations. The strong seasonality described above is present and the residual is a stationary series. The analysis shows an especially high value of precipitation observed for the year 2018, which is supported by the ground station data at least compared to the other available years. The long-term average value is consistently positive across two decades and falls between 0.04 and 0.15 mm/hr.

Figure 6: Time series decomposition of a 20-year monthly rainfall rate time series from the IMERG v6 dataset over Longido (top row), showing the 12-month running mean (second row), seasonal component (third row), and residuals (bottom row).



In an effort to comprehend the behaviour of precipitation across the time period of interest, the time series were examined for correlations with common climate modes. According to the Oceanic Niño Index (ONI), over the past two decades, the years 1997-1998 and 2015-2016 witnessed very strong ENSO phases, whereas 2018 was a neutral year. However, the Dipole Mode Index (DMI) which indicates the east-west temperature gradient across the tropical Indian Ocean, and therefore the strength of the Indian Ocean Dipole (IOD), shows that 2018 had an enhanced IOD. The correlation coefficient of the running mean component of the precipitation time series against the monthly Niño 3.4 index is 0.16 (95% confidence interval from 0.04 to 0.28), and against the monthly DMI is 0.22 (95% confidence interval from 0.09 to 0.33).

The high precipitation in 2018 does coincide with a rare instance where five storm systems were observed simultaneously in the southern Indian Ocean. Rowell (2019) suggests a relationship between the sea-surface temperatures (SST) in the southern Indian Ocean and the net cloud radiative effect over Eastern Africa and moisture transport to that region. The present study provides confirmation of high precipitation accumulation on the ground in Tanzania during the 2018 event. The relationship between southern Indian Ocean SST and the East African long rains does suggest an increase of about a third in rainfall accumulation by the end of the 21st century.

CONCLUSIONS

Rainfall data from a ground station in Longido, Tanzania, was compared with satellite-retrieved precipitation values from the GPM mission's IMERG v6 product. Seasonally, rainfall in Eastern Africa follows a bimodal pattern, in which the long rains of March through May contribute most of the annual precipitation and the short rains in October through December the rest with only sparse rainfall at other times of the year. We find at Longido that the long rain accumulation is highly variable from year to year, with totals between 12.2 mm (April

2019) and 238 mm (March 2018). The peak accumulation recorded by the ground station during the short rain season was 63 mm (November 2017).

Specific rainfall events also vary substantially, as is demonstrated by the maximum hourly rainfall rate and 90th percentile daily mean rate. The highest hourly rate recorded for the entire record was 22 mm/hr (January 2016), while the month with the highest 90th percentile daily mean rate was March 2018 (980 $\mu\text{m/hr}$). Both March and April 2018 saw very high rainfall compared to other years on record. The IMERG data confirms that these months particularly are the highest of the decade. 2018 was a neutral year regarding ENSO but showed a highly active Indian Ocean Dipole and high SSTs in the southern Indian Ocean, both of which are linked to enhanced precipitation during the long rains of Eastern Africa.

The IMERG data shows promise in representing the variability of precipitation in Eastern Africa at monthly timescales; however, the data does have a slightly high bias and significantly overestimates the frequency of heavy rainfall events (> 10 mm/hr) compared to low-intensity events (< 2 mm/hr) and is not recommended for analysis at daily scales.

The behaviour of monthly precipitation in Longido over two decades of IMERG data shows a distinct double-peaked seasonal cycle, with long rains in March and April and short rains in November and December. Time series analysis using an additive model of a long-term average and a seasonal cycle produces stationary residuals and modest correlations were found between the monthly precipitation time series and the Niño 3.4 index and the Indian Ocean Dipole. A more robust predictive model remains elusive.

ACKNOWLEDGMENTS

Funding for this project was provided by Carleton University. The authors would also like to acknowledge TEMBO (Tanzanian Education and Micro Business Opportunity) for supporting the

project and in particular, Christina Sumayani who assisted with local weather station data collection.

The IMERG version 06B level 3 data were provided by the NASA/Goddard Space Flight Center's GPM and PPS, which develop and compute the IMERG data as a contribution to GPM and archived at the NASA GES DISC. WMO Climatological Normals were obtained from <http://worldweather.wmo.int/en/country.html?countryCode=TZA>. The Niño 3.4 index and the Dipole Mode Index were obtained from NOAA: https://psl.noaa.gov/gcos_wgsp/Timeseries/Data/.

REFERENCES

- Bates, B. C., Kundzewicz, Z. W., Wu, S., and Palutikof, J. P. (2008). Climate Change and Water. Technical report, Intergovernmental Panel on Climate Change, IPCC Secretariat, Geneva, Switzerland. URL: <https://www.ipcc.ch/publication/climate-change-and-water-2/>
- Chakraborty, A., Nanjundiah, R. S., and Srinivasan, J. (2009). Impact of African orography and the Indian summer monsoon on the low-level Somali jet. *International Journal of Climatology*, 29(7):983–992. DOI: <https://doi.org/10.1002/joc.1720>
- Dyer, E. L. E., Jones, D. B. A., Li, R., Sawaoka, H., and Mudryk, L. (2017). Sahel precipitation and regional teleconnections with the Indian Ocean. *J. Geophys. Res. Atmos.*, 122:5654–5676. DOI: <https://doi.org/10.1002/2016JD026014>
- Gilewski, P. and Nawalany, M. (2018). Inter-Comparison of Rain-Gauge, Radar, Satellite (IMERG GPM) Precipitation Estimates Performance for Rainfall-Runoff Modeling in a Mountainous Catchment in Poland. *Water*, 10:1665–1688. DOI: <https://doi.org/10.3390/w10111665>
- Hou, A. Y., Kakar, R. K., Neeck, S., Azarbarzin, A. A., Kummerow, C. D., Kojima, M., Oki, R., Nakamura, K., and Iguchi, T. (2014). The Global Precipitation Measurement Mission. *Bull. Amer. Meteor. Soc.*, 95(5):701–722. DOI: <https://doi.org/10.1175/BAMS-D-13-00164.1>
- Huffman, G. J., Bolvin, D. T., Braithwaite, D., Hsu, K., Joyce, R., Kidd, C., Nelkin, E. J., Sorooshian, S., Tan, J., and Xie, P. (2019a). NASA Global Precipitation Measurement Integrated Multi-satellite Retrievals for GPM (IMERG) Algorithm Theoretical Basis Document, V06. Technical report, NASA Goddard Space Flight Center. URL: <https://gpm.nasa.gov/resources/documents/algorithm-information/IMERG-V06-ATBD>
- Huffman, G. J., Stocker, E. F., Bolvin, D. T., Nelkin, E., and Tan, J. (2019b). GPM IMERG Final Precipitation L3 1 day 0.1-degree x 0.1 degree V06. Goddard Earth Sciences Data and Information Services Center (GES DISC), accessed March, 2020, https://disc.gsfc.nasa.gov/datasets/GPM_3IME_RGM_06/.
- Hunziker, S., Gubler, S., Calle, J., Moreno, I., Andrade, M., Velarde, F., Ticona, L., Carrasco, G., Castellón, Y., Oria, C., Croci-Maspoli, M., Konzelmann, T., Rohrer, M., and Brönnimann, S. (2017). Identifying, attributing, and overcoming common data quality issues of manned station observations. *International Journal of Climatology*, 37(11):4131–4145. DOI: <https://doi.org/10.1002/joc.5037>
- Li, Z., Chen, M., Gao, S., Hong, Z., Tang, G., Wen, Y., Gourley, J. J., and Hong, Y. (2020). Cross-Examination of Similarity, Difference and Deficiency of Gauge, Radar and Satellite Precipitation Measuring Uncertainties for Extreme Events Using Conventional Metrics and Multiplicative Triple Collocation. *Remote Sensing*, 12:1258–1276. DOI: <https://doi.org/10.3390/rs12081258>

- Lyon, B. (2014). Seasonal drought in the Greater Horn of Africa and its recent increase during the March–May long rains. *J. Clim.*, 27:7953–7976. DOI: <https://doi.org/10.1175/JCLI-D-13-00459.1>
- Matayo, I., Semazzi, F., and Xie, L. (2000). Mechanistic model simulations of the East African climate using NCAR regional climate model: Influence of large-scale orography on the Turkana Low-level Jet. *J. Clim.*, 14:2710–2724. DOI: [https://doi.org/10.1175/1520-0442\(2001\)014%3C2710:MMSOTE%3E2.0.CO;2](https://doi.org/10.1175/1520-0442(2001)014%3C2710:MMSOTE%3E2.0.CO;2)
- Mkonda, M. Y. and He, X. (2018). Climate variability and crop yields synergies in Tanzania’s semi-arid agroecological zone. *Ecosystem Health and Sustainability*, 4(3):59–72. DOI: <https://doi.org/10.1080/20964129.2018.1459868>
- Nicholson, S. (2016). The Turkana low-level jet: mean climatology and association with regional aridity. *International Journal of Climatology*, 36(6):2598–2614. DOI: <https://doi.org/10.1002/joc.4515>
- Nicholson, S. E. and Klotter, D. (2020). The Tropical Easterly Jet over Africa, its representation in six reanalysis products, and its association with Sahel rainfall. *International Journal of Climatology*, 41(1):328–347. DOI: <https://doi.org/10.1002/joc.6623>
- O, S., Foelsche, U., Kirchengast, G., Fuchsberger, J., and Tan, J. (2017). Evaluation of GPM IMERG Early, Late, and Final rainfall estimates using WegenerNet gauge data in southeastern Austria. *Hydrology and Earth System Sciences*, 21(12):6559–6548. DOI: <https://doi.org/10.5194/hess-21-6559-2017>
- Ogwang, B. A., Huberg, K., Cheikh, D., and Kamga, A. (2019). The State of Climate of Africa in 2018. Technical report, African Center of Meteorological Applications for Development.
- Rowell, D. P. (2019). An Observational Constraint on CMIP5 Projections of the East African Long Rains and Southern Indian Ocean Warming. *Geophys. Res. Lett.*, 46:6050–6058. DOI: <https://doi.org/10.1029/2019GL082847>
- Skofronick-Jackson, G., Kirschbaum, D., Petersen, W., Huffman, G., Kidd, C., Stocker, E., and Kakar, R. (2018). The Global Precipitation Measurement mission’s scientific achievements and societal contributions: reviewing four years of advanced rain and snow observations. *Q. J. R. Meteorol. Soc.*, 144(S1):27–48. DOI: <https://doi.org/10.1002/qj.3313>
- Slingo, J., Spencer, H., Hoskins, B., Berrisford, P., and Black, E. (2005). The meteorology of the Western Indian Ocean, and the influence of the East African Highlands. *Philosophical Transactions of the Royal Society A: Mathematical, Physical and Engineering Sciences*, 363(1826):25–42. DOI: <https://doi.org/10.1098/rsta.2004.1473>
- Takaya, Y., Kosaka, Y., Watanabe, M., and Maeda, S. (2021). Skilful predictions of the Asian summer monsoon one year ahead. *Nature Communications*, 12:2094–2102. DOI: <https://doi.org/10.1038/s41467-021-22299-6>
- Thiery, W., Brussel, V. U., Demuzere, M., and Lhermitte, S. (2015). The impact of the African Great Lakes on the regional climate. *J. Clim.*, 28:4061–4084. DOI: <https://doi.org/10.1175/JCLI-D-14-00565.1>
- Walker, D., Forsythe, N., Parkin, G., and Gowing, J. (2016). Filling the observational void: Scientific value and quantitative validation of hydrometeorological data from a community-based monitoring programme. *Journal of Hydrology*, 538:713–725. DOI: <https://doi.org/10.1016/j.jhydrol.2016.04.062>

Yang, W., Seager, R., Cane, M., and Lyon, B. (2015). The annual cycle of East African precipitation. *J. Clim.*, 28:2385–2405. DOI: <https://doi.org/10.1175/JCLI-D-14-00484.1>